Observing and Modeling of Solar Coronal Structures Using High-Resolution Eclipse Images and Space-based Telescopes with Wide Field-of-View

SOLAR PHYSICS 2013 MEETING — SPD Student Poster Award candidate

#100.25

Muzhou Lu[1], Jay M. Pasachoff[1], Yingna Su[2], Aad van Ballegooijen[2], Daniel B. Seaton[3], Matthew West[3]

[1]Williams College, Williamstown, MA, [2]Harvard-Smithsonian Center for Astrophysics, Cambridge, MA, [3]Solar Influences Data Analysis Center, Royal Observatory of Belgium

ABSTRACT

We present a comparison of the solar corona observed during the total solar eclipses on 2010 July 11 and on 2012 November 13. The white light images were taken at Easter Island in 2010 and at Northeast Queensland, Australia, in 2012; while the concurrent EUV images were take with SDO/AIA and PROBA2/SWAP. The 2010 eclipse was observed at the beginning of Sunspot Cycle 24 [1], which peaked near our 2012 observation. We compare a plethora of corona features in the white light images and reveal some interesting differences in the enhanced EUV images taken by SDO/AIA and PROBA2/SWAP. We construct potential field models using our newly refined Coronal Modeling System (CMS2) software with line-of-sight photospheric magnetograms from SDO/HMI. The source surface heights derived from detailed comparison between our models and observations are compared to the standard source-surface model. We also compare the dynamics of the two eclipse observations. Similar to the 2010 eclipse, a CME was observed at the 2012 eclipse using temporally spaced eclipse images. We address unresolved problems in the models and observations with the hope of correcting them for future eclipse observations, such as the 2017 total solar eclipse across the continental U.S.

Eclipse Observations & Composite Eclipse Images

Image Registration Techniques:

- Adaptive Circular (or Tangential) High-pass Filter (ACHF) and phase-correlation
  - Preserves high spatial frequency in tangential direction by means of a Gaussian kernel
  - Extracted Fourier spectra of the images differ only in the phase
  - A composite image with 8 bits per pixel can cover a typical range of 0-10^6
- Normalizing-Radial-Graded Filter (NRGF)
  - Reduce the radial gradient at every latitudinal section
  - The image intensity is normalized to a mean of zero and a standard deviation of one
- Fourier Normalizing-Radial-Graded Filter (FNRGF)
  - The average pixel value and standard deviation are calculated for each cell
  - Tenth-order Fourier series to approximate the average and standard deviation functions

Image on the right shows the computational domain of the FNRGF. The latitudinal sections are smaller and more numerous (n is large), while the annuli are one pixel wide each. (Druckmüllerová, Morgan, & Habbal 2011, Fig. 1a.)

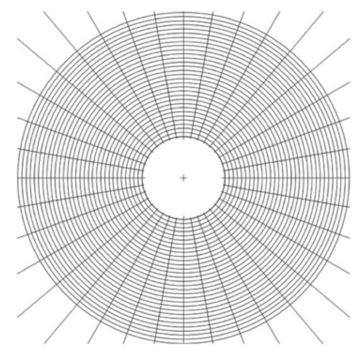

2010

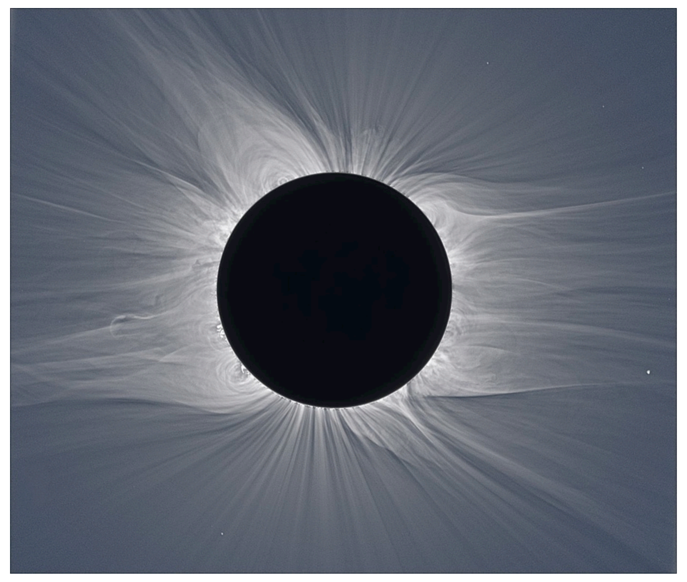

Left is a composite image, made from 73 individual frames using the ACHF and phase-correlation method, showing the total phase of the 2010 July 11 eclipse, viewed from Easter Island. Individual frames were taken by a Nikon D90 dSLR camera with a Nikkor 500mm lens. (Jay M. Pasachoff, Hana Druckmüllerová, Bryce A. Babcock, and Muzhou Lu.)

2012

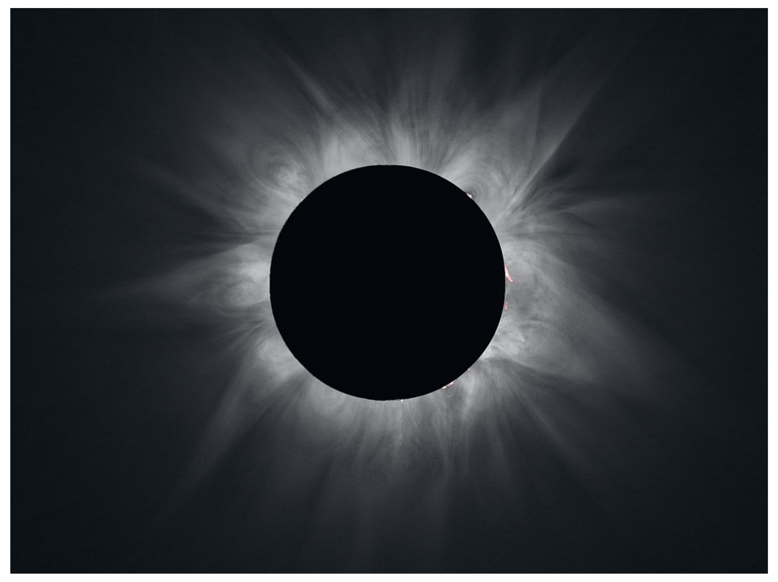

Left is a composite image (b), made from 58 individual frames, showing the total phase of the 2012 November 13 eclipse, viewed from Queensland, Australia. Individual frames were taken by a Red Epic camera with a Takahashi FSQ telescope. (Paul Gaintatzis (Aristotle University of Thessaloniki, Greece), and Ronald Dantowitz and Nicholas Weber (Clay Center Observatory, Dexter Southfield School).)

Space-based Observations from SDO/AIA, SDO/HMI and PROBA2/SWAP

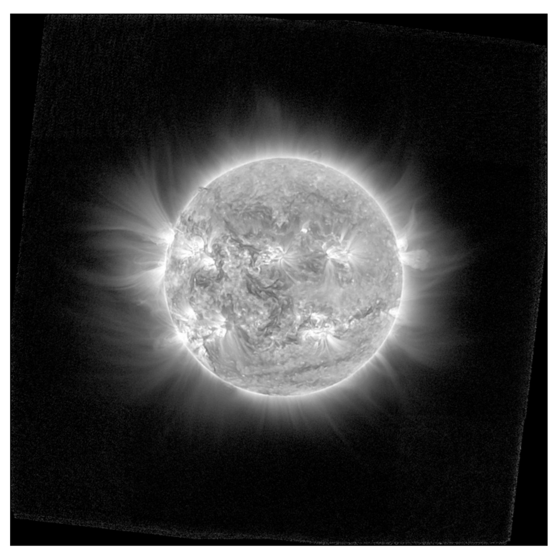

Radial-filtered SWAP mosaic, using off-pointed images in the 174-Å passband. (M. Lu and D. B. Seaton, SIDC/ROB.)

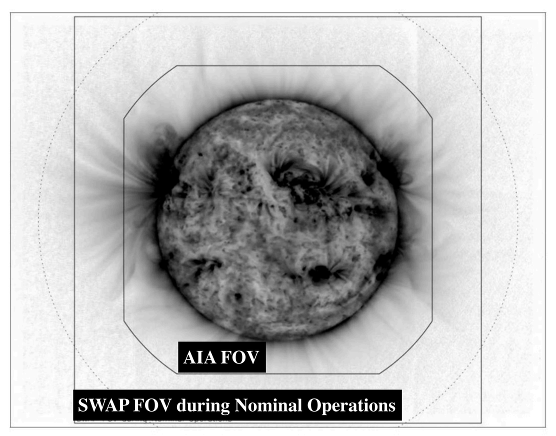

A SWAP mosaic image (seen in inverted color) showing the extent of the EUV corona on 2011 September 19. SWAP has a bigger FOV than AIA and can easily off-point to increase its FOV near 2 $R_\odot$ (shown as the dotted circle). This can be essential when studying off-limb structures. Although SWAP has its own "eclipse seasons," it can provide images during SDO data dropouts. (Seaton, et al. 2013, Fig. 9, with permission from author.)

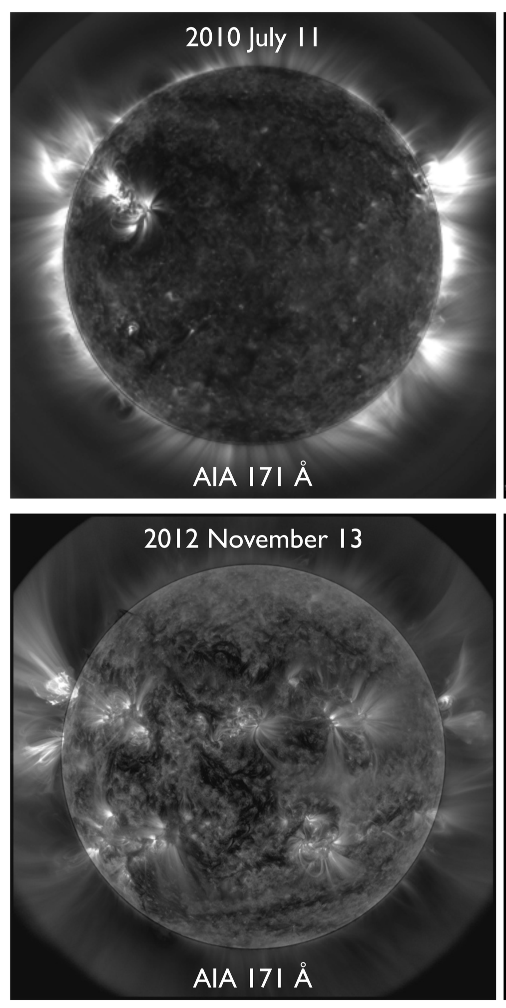

Radial-filtered AIA images in 171 Å (~1 MK) taken at 20:38:05 UT. FOV is limited to 1.28 $R_\odot$. (SDO/LMSAL/NASA.)

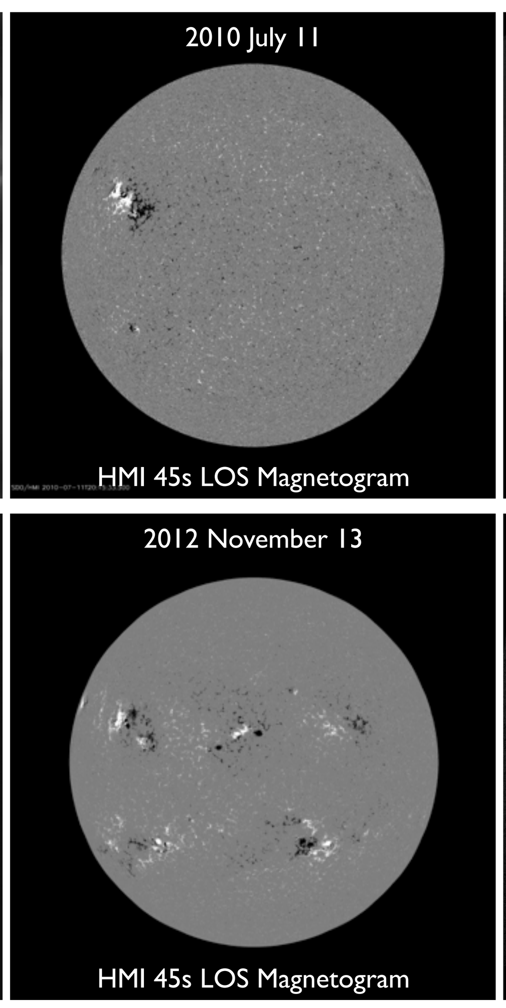

HMI 45-s line-of-sight magnetograms showing spatial distribution of the photospheric magnetic field. (SDO/LMSAL/NASA.)

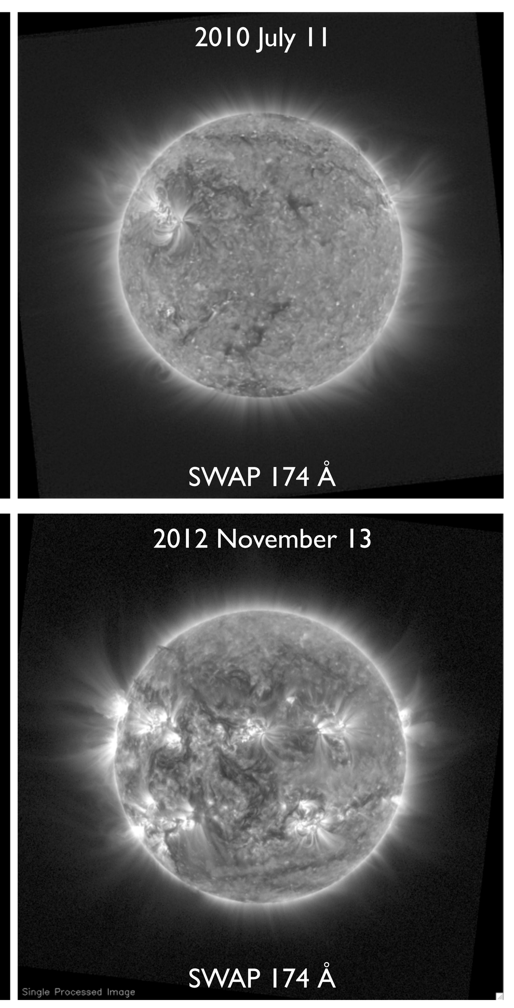

Radial-filtered SWAP images in the 174-Å passband taken at ~20:39 UT. (M. Lu and D. B. Seaton, SIDC/ROB.)

Constructing Potential Field Models

Step One: Construct a map of the radial magnetic field B_r ($R_\odot$, θ, φ) as a function of longitude and latitude on the solar surface ($r = R_\odot$). This map can be constructed from one or more magnetograms.

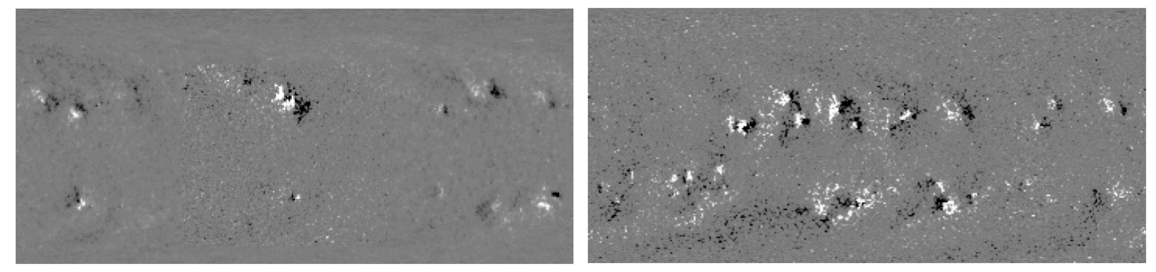

Processed magnetogram of Carrington rotation 2098 (left) and 2130 (right) using global synoptic maps and high-res regions of four combined HMI 45-s LOS magnetograms for 2010 data (left) and five for 2012 data (right). (NSO/SOLIS, SDO/HMI, processed in CMS2.)

Step Two: Apply spherical-harmonics expansion (fitting the coefficients of expansion terms based on observed magnetic field data) to the global magnetogram. The combined lower-res synoptic data and HMI's high-res LOS magnetograms can improve the fit of our model.

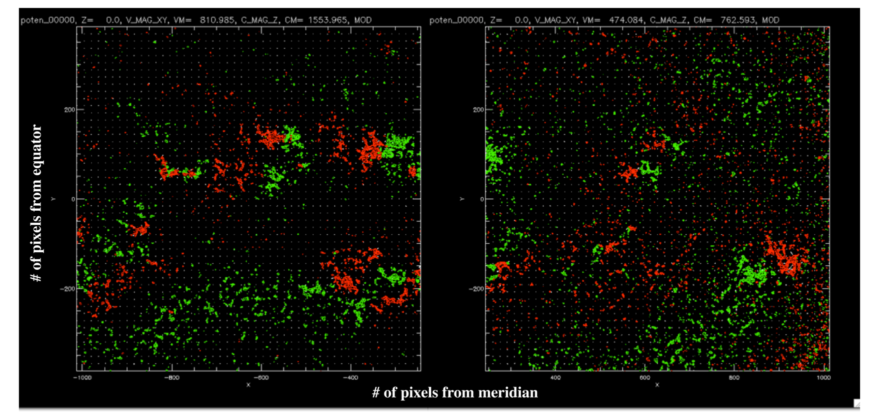

A comparison between the east limb (left) and west limb (right) models in the 2012 data. Each image shows the computed potential magnetic field map of the high-res regions. (Processed in CMS2.)

Limitations of Our Potential Field Models:

- The radial magnetic field, B_r ($R_\odot$, θ, φ), is computed from the line-of-sight data using $B_r = B_\parallel/\cos\theta_C$, where θ_C is the heliocentric angle. This formula is accurate only when the observed field is radial on the Sun, and when we observe near the center of solar disk. This prevents an accurate description of the magnetic field in sunspot penumbrae away from disk center because the field there has a strong horizontal component. For what we are studying, the large structure over the quiet region or across sunspot groups, this LOS-to-radial field extraction is reasonably accurate.
- The best way to model magnetic features observed near the limb during eclipses is to use HMI's high-resolution line-of-sight magnetograms from a few days before (for west-limb models) and after (for east-limb models) the time of the eclipse and select the region near the center of the solar disk. This method sets the temporal resolution of our model and limits the type of dynamical events that can be studied.

Comparing Potential Field Models and Observations

- We used three source surface values: 1.616 $R_\odot$ and 2.560 $R_\odot$ (based on the standard PFSS models suggested by Schatten and Wilcox (1968) and Altschuler and Newkirk (1969)) and 2.014 $R_\odot$.
- 2010 models show that $R_{ss} = 1.616\ R_\odot$ is a better fit than $R_{ss} = 2.560\ R_\odot$; whereas 2012 models show that $R_{ss} = 2.560\ R_\odot$ is a better fit than $R_{ss} = 1.616\ R_\odot$.
- More models matching future eclipse data are needed to establish a more accurate fit for the height of the source surface.
- Difference in 2010 and 2012 model fit suggests a link between the source-surface height and overall activity level in the solar corona.
- The rising solar cycle should generally drive increasing nonpotentiality in the corona. As structures become more complex, more energy is stored in nonpotential loops and other structures, meaning the potential field models will work poorly regardless of surface height.
- The source-surface height for the best fit will probably increase due to increasing solar activity.

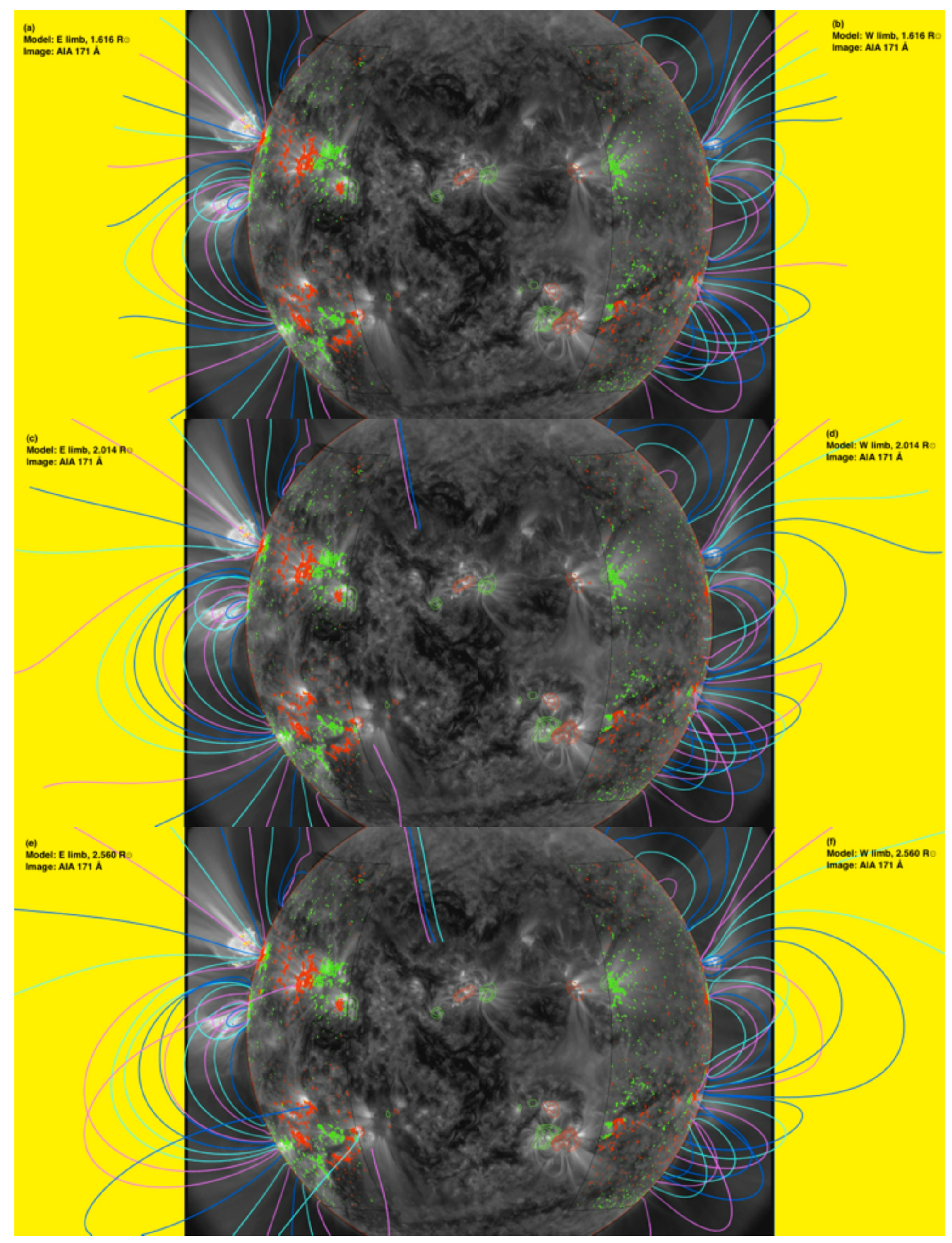

Six different potential field models of the solar corona shown at 2012-11-13 20:39:00 UT. (a), (c), and (e) represent the field configuration over the east limb during the eclipse, while (b), (d), and (f) represent the west limb. (a) and (b) have $R_{ss} = 1.616\ R_\odot$; (c) and (d) have $R_{ss} = 2.014\ R_\odot$; and (e) and (f) have $R_{ss} = 2.560\ R_\odot$. The yellow region is outside AIA's FOV. (SDO/AIA, CMS2 3D Display.)

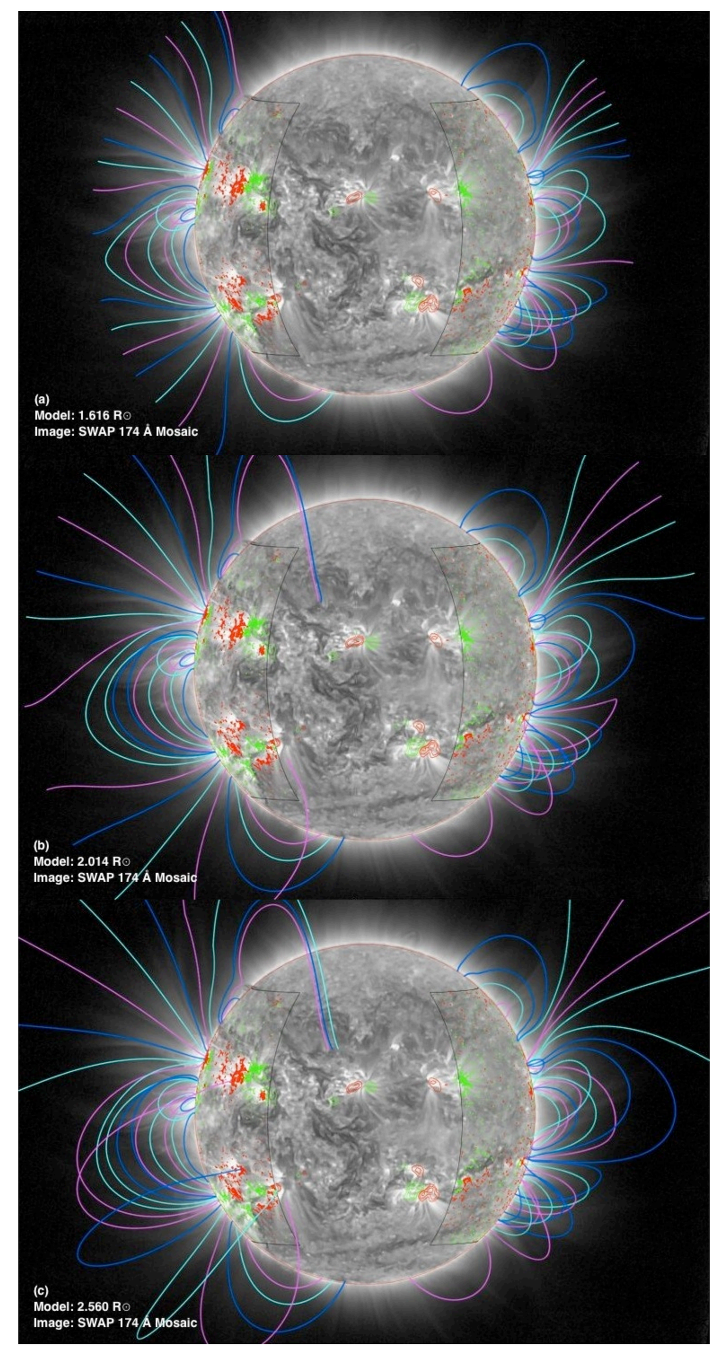

Each image combines two separate models of the east and west limb, showing the magnetic field configuration with source surfaces at $R_{ss} = 1.616\ R_\odot$ (a), $R_{ss} = 2.014\ R_\odot$ (b), and $R_{ss} = 2.560\ R_\odot$ (c). (PROBA2/SWAP, CMS2 3D Display.)

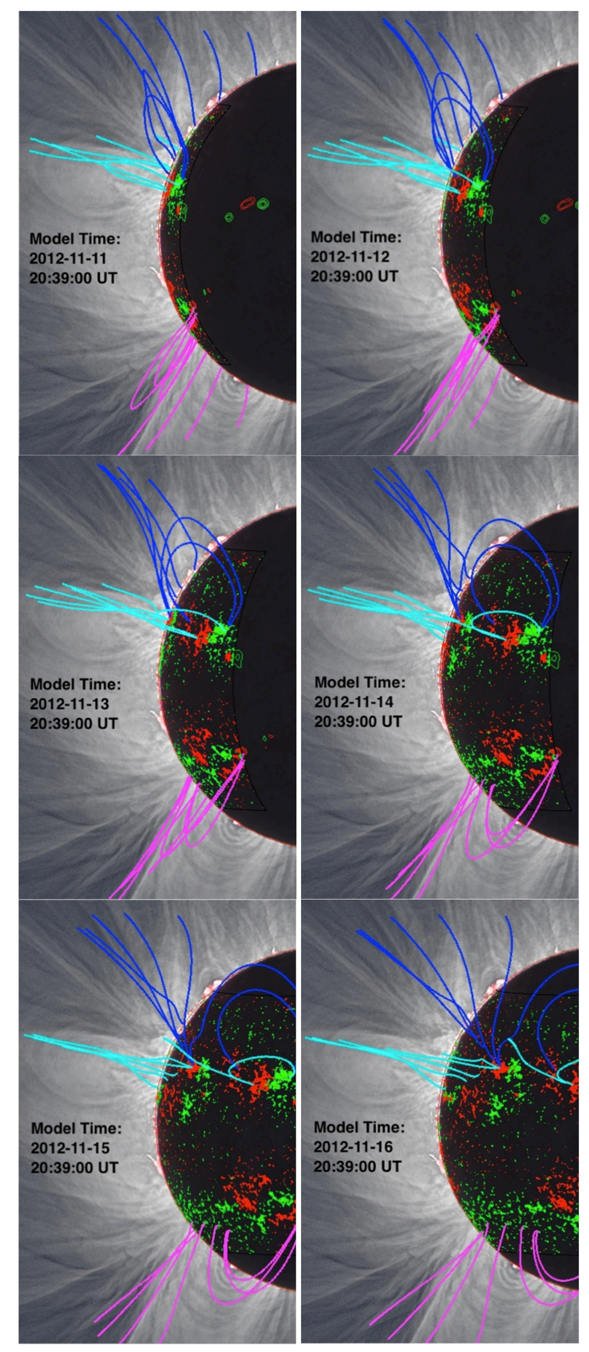

East limb model ($R_{ss} = 2.014\ R_\odot$) shown in 6 frames during the 2012-11-13 eclipse at 20:39:00 UT. The model spans 90° in the longitudinal direction. (C. Emmanouilidis, M. Druckmüller, CMS2 3D Display.)

Acknowledgments: We thank Craig Malamut, Ronald Dantowitz, and Nicolas Weber for observational support. We thank Hana Druckmüllerová and Pavlos Gaintazis for image processing. We also thank Karen Kwitter for draft revision and David Berghmans for SWAP-related help. The 2012 eclipse observations and analysis of the 2010 results were supported in part by the Solar-Terrestrial Program of the Atmospheric and Geospace Sciences Division of the National Science Foundation through grant AGS- 1047726; the 2010 and 2012 expedition received additional support from the Brandi Fund, the Rob Spring Fund, and the Science Center funds from Williams College. ML's 2012 eclipse expedition was funded in part by a *Grant-In-Aid of Research* from the National Academy of Sciences, administered by Sigma Xi, The Scientific Research Society (Grant ID: G201203151599311). ML's participation in the PROBA2/SWAP investigation was supported by a GI (Guest Investigator) Grant through the PROBA2 Science Center.

Select References:

[1] Pasachoff, J. M., Rusin, V., Druckmüllerová, H., Saniga, M., Lu, M., Malamut, C., Seaton, D. B., Golub, L., Engell, A. J., Hill, S. W., Lucas, R., 2011, *Astrophysical Journal*, **734**, 114

[2] Lu, M., & Malamut, C. 2010, "High- Resolution Imaging of the 2010 Total Solar Eclipse at Easter Island," in Keck Northeast Astronomy Consortium: 2010, ed. D. Cohen (Colgate University)

[3] Seaton, D. B., et al. 2013, *Solar Physics*, **286,** 23

[4] Druckmüllerová, H., Morgan, H., & Habbal, S. R. 2011, *Astrophysical Journal*, **737,** 10

[5] Golub, L., & Pasachoff, J. M. 2010, *The Solar Corona* (2nd ed.: Cambridge University Press, New York)

[6] Altschuler, M. D., & Newkirk, G. 1969, *Solar Physics*, **9,** 19

[7] Schatten, K. H., & Wilcox, J. M. 1968, *Solar Physics*, **6,** 14

2013 SPD Meeting, Bozeman, Montana. For more information contact Muzhou Lu at ml4@williams.edu